International Journal of Modern Physics A
© World Scientific Publishing Company

arXiv:1407.0916v1 [hep-ph] 3 Jul 2014

PROBING NEW PHYSICS WITH $B_s^0 \to \mu^+\mu^-$: STATUS AND PERSPECTIVES

ROBERT FLEISCHER

Nikhef, Science Park 105, NL-1098 XG Amsterdam, Netherlands
Department of Physics and Astronomy, Vrije Universiteit Amsterdam,
NL-1081 HV Amsterdam, Netherlands
Robert.Fleischer@nikhef.nl

The rare decay $B_s^0 \to \mu^+\mu^-$ plays a key role for the testing of the Standard Model. It is pointed out that the sizable decay width difference $\Delta\Gamma_s$ of the B_s-meson system affects this channel in a subtle way. As a consequence, its calculated Standard Model branching ratio has to be upscaled by about 10%. Moreover, the sizable $\Delta\Gamma_s$ makes a new observable through the effective $B_s^0 \to \mu^+\mu^-$ lifetime accessible, which probes New Physics in a way complementary to the branching ratio and adds an exciting new topic to the agenda for the high-luminosity upgrade of the LHC. Further probes of New Physics are offered by a CP-violating rate asymmetry. Correlations between these observables and the $B_s^0 \to \mu^+\mu^-$ branching ratio are illustrated for specific models of New Physics.

Keywords: Rare B decays, New Physics.

PACS numbers: 13.20.He, 12.60.-i

1. Introduction

In the Standard Model (SM), the decay $B_s^0 \to \mu^+\mu^-$ arises only from loop contributions related to penguin and box topologies, as can be seen in Fig. 1, and is helicity suppressed, resulting in a strongly suppressed branching ratio which is proportional to m_μ^2. As only leptons are present in the final state, the hadronic sector is very simple and described by a single non-perturbative parameter, the B_s decay constant F_{B_s}, which is defined through the relation

$$\langle 0|\bar{b}\gamma_5\gamma_\mu s|B_s^0(p)\rangle = iF_{B_s}p_\mu. \tag{1}$$

In view of these features, $B_s^0 \to \mu^+\mu^-$ belongs to the cleanest rare B decays Nature has to offer and represents an outstanding probe for physics beyond the SM.

In the SM, the parametric dependence on the relevant input parameters is given as follows:[1,2]

$$\begin{aligned}\mathrm{BR}(B_s \to \mu^+\mu^-)_{\mathrm{SM}} &= 3.25 \times 10^{-9} \\ &\times \left[\frac{M_t}{173.2\,\mathrm{GeV}}\right]^{3.07} \left[\frac{F_{B_s}}{225\,\mathrm{MeV}}\right]^2 \left[\frac{\tau_{B_s}}{1.500\mathrm{ps}}\right] \left|\frac{V_{tb}^*V_{ts}}{0.0405}\right|^2,\end{aligned} \tag{2}$$

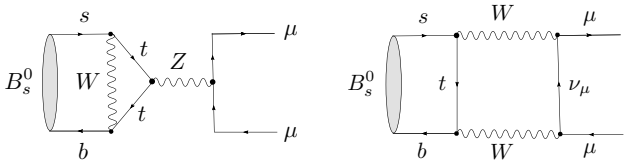

Fig. 1. Penguin and box diagrams contributing to the $B_s^0 \to \mu^+\mu^-$ decay in the Standard Model.

where M_t is the top-quark mass, τ_{B_s} the B_s^0-meson lifetime, and $V_{tb}^* V_{ts}$ the relevant combination of elements of the Cabibbo–Kobayashi–Maskawa (CKM) matrix.

Concerning the SM prediction of the $B_s^0 \to \mu^+\mu^-$ branching ratio, there has recently been important progress in lattice QCD,[3] which is reflected by the result $F_{B_s} = (227.7 \pm 4.5)$ MeV, while progress on the experimental side[4] led to an improved measurement of $\tau_{B_s} = (1.516 \pm 0.011)$ ps. In Fig. 2, the corresponding error budget for the SM value of the $B_s^0 \to \mu^+\mu^-$ branching ratio is shown. On the theoretical side,[5] there was important progress thanks to a very impressive calculation of NLO electroweak effects[6] and NNLO QCD matching corrections,[7] resulting in

$$\mathrm{BR}(B_s \to \mu^+\mu^-)_{\mathrm{SM}} = (3.38 \pm 0.22) \times 10^{-9}, \tag{3}$$

which supersedes the prediction in Ref. 2.

Thanks to the impact of New Physics (NP), i.e. physics beyond the SM, the branching ratios of the $B_{s,d}^0 \to \mu^+\mu^-$ decays could have been enhanced significantly, in particular in supersymmetric flavor models (see, for instance, Refs. 8, 9 and references therein). In view of this feature, there was the exciting possibility to observe $B_s^0 \to \mu^+\mu^-$ already at the Tevatron in the previous decade. As the Tevatron collider is now legacy, the CDF and D0 collaborations have presented their final results on the search for $B_s^0 \to \mu^+\mu^-$, corresponding to the 95% C.L. upper bounds 15×10^{-9} and 31×10^{-9}, respectively.[10,11]

The analysis of the rare $B_s^0 \to \mu^+\mu^-$ channel is now conducted at the Large Hadron Collider (LHC). The ATLAS experiment[12] has set the upper bound $\mathrm{BR}(B_s \to \mu^+\mu^-) < 15 \times 10^{-9}$ (95% C.L.), while the *first evidence* for $B_s^0 \to \mu^+\mu^-$ was reported by the CMS[13] and LHCb[14] collaborations in 2013, with the results

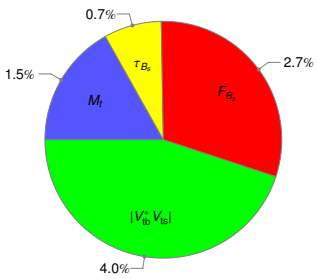

Fig. 2. The error budget of $\mathrm{BR}(B_s \to \mu^+\mu^-)_{\mathrm{SM}}$ related to the various input parameters.[2]

$\mathrm{BR}(B_s \to \mu^+\mu^-) = (3.0^{+1.0}_{-0.9}) \times 10^{-9}$ and $(2.9^{+1.1}_{-1.0}) \times 10^{-9}$, respectively. The average of these LHC measurements is given as follows:[15]

$$\mathrm{BR}(B_s \to \mu^+\mu^-) = (2.9 \pm 0.7) \times 10^{-9}. \tag{4}$$

It should be noted that the limiting factor for the $\mathrm{BR}(B_s \to \mu^+\mu^-)$ measurement – and actually all B_s branching ratios – is given by the ratio f_s/f_d of the corresponding fragmentation functions.[16,17]

It will be interesting to keep an eye on $B_d^0 \to \mu^+\mu^-$. The current information on the branching ratio reported by the CMS and LHCb collaborations is given by

$$\mathrm{BR}(B_d \to \mu^+\mu^-) = \begin{cases} (3.5^{+2.1}_{-1.8}) \times 10^{-10} < 11 \times 10^{-10} & \text{(CMS)} \\ (3.7^{+2.4}_{-2.1}) \times 10^{-10} < 7.4 \times 10^{-10} & \text{(LHCb),} \end{cases} \tag{5}$$

where the upper bounds refer to the 95% C.L., resulting in the LHC average[15]

$$\mathrm{BR}(B_d \to \mu^+\mu^-) = (3.6^{+1.6}_{-1.4}) \times 10^{-10}. \tag{6}$$

On the other hand, the SM prediction is given as follows:[5]

$$\mathrm{BR}(B_d \to \mu^+\mu^-)_{\mathrm{SM}} = (1.06 \pm 0.09) \times 10^{-10}. \tag{7}$$

The current experimental errors are too big to draw conclusions about physics beyond the SM model. However, should a result around the central value in (6) be established in the future, it would immediately rule out the SM and its extensions with "Minimal Flavor Violation" (MFV).

2. Branching Ratios of B_s Decays for $\Delta\Gamma_s \neq 0$

Thanks to B_s^0–$\bar{B}_s^0$ mixing, an initially, i.e. at time $t = 0$, present B_s^0 meson evolves into a time-dependent linear combination of $|B_s^0\rangle$ and $|\bar{B}_s^0\rangle$ states:[18]

$$|B_s(t)\rangle = a(t)|B_s^0\rangle + b(t)|\bar{B}_s^0\rangle. \tag{8}$$

The time evolution is described by an appropriate Schördinger equation. It is solved by introducing mass eigenstates B_s^{H} ("heavy") and B_s^{L} ("light") which are characterised by the differences

$$\Delta M_s \equiv M_{\mathrm{H}}^{(s)} - M_{\mathrm{L}}^{(s)} \quad \text{and} \quad \Delta\Gamma_s \equiv \Gamma_{\mathrm{L}}^{(s)} - \Gamma_{\mathrm{H}}^{(s)} \tag{9}$$

of their masses and decay widths, respectively. A characteristic feature of the B_s-meson system is a sizeable decay width difference $\Delta\Gamma_s$, which has been expected on theoretical grounds since decades; for a recent review, see Ref. 19. In contrast, the decay width difference of the B_d-meson system is negligibly small. Recently, a non-zero value of $\Delta\Gamma_s$ has actually been established at the $6\,\sigma$ level by LHCb:[20]

$$y_s \equiv \frac{\Delta\Gamma_s}{2\,\Gamma_s} \equiv \frac{\Gamma_{\mathrm{L}}^{(s)} - \Gamma_{\mathrm{H}}^{(s)}}{2\,\Gamma_s} = 0.075 \pm 0.012, \tag{10}$$

where the decay width parameter y_s characterises the impact of $\Delta\Gamma_s$ in formulae to be given below.

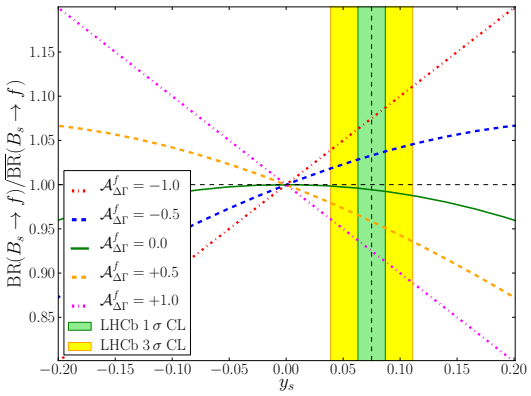

Fig. 3. The ratio of the theoretical to the experimental branching ratio of $B_s \to f$ as a function of the decay width parameter y_s for various values of the observable $\mathcal{A}^f_{\Delta\Gamma}$.

In view of the sizeable decay width difference $\Delta\Gamma_s$ special care has to be taken when dealing with branching ratios of B_s-meson decays.[21,22] The starting point for the analysis of branching ratios is the following "untagged" rate, where no distinction between initially, i.e. at time $t = 0$, present B^0_s or $\bar{B}^0_s$ mesons is made:

$$\langle \Gamma(B_s(t) \to f)\rangle \equiv \Gamma(B^0_s(t) \to f) + \Gamma(\bar{B}^0_s(t) \to f) = R^f_{\rm H} e^{-\Gamma^{(s)}_{\rm H} t} + R^f_{\rm L} e^{-\Gamma^{(s)}_{\rm L} t}$$

$$= \left(R^f_{\rm H} + R^f_{\rm L}\right) e^{-\Gamma_s t} \left[\cosh\left(\frac{y_s\, t}{\tau_{B_s}}\right) + \mathcal{A}^f_{\Delta\Gamma} \sinh\left(\frac{y_s\, t}{\tau_{B_s}}\right)\right]. \tag{11}$$

The "experimental" branching ratio refers to the time-integrated untagged rate:[23]

$$\mathrm{BR}\,(B_s \to f)_{\rm exp} \equiv \overline{\mathrm{BR}}\,(B_s \to f) \equiv \frac{1}{2}\int_0^\infty \langle \Gamma(B_s(t) \to f)\rangle\, dt$$

$$= \frac{1}{2}\left[\frac{R^f_{\rm H}}{\Gamma^{(s)}_{\rm H}} + \frac{R^f_{\rm L}}{\Gamma^{(s)}_{\rm L}}\right] = \frac{\tau_{B_s}}{2}\left(R^f_{\rm H} + R^f_{\rm L}\right)\left[\frac{1 + \mathcal{A}^f_{\Delta\Gamma}\, y_s}{1 - y_s^2}\right]. \tag{12}$$

On the other hand, in theoretical analyses, usually the following "theoretical" branching ratio is considered:[24–26]

$$\mathrm{BR}\,(B_s \to f) \equiv \frac{\tau_{B_s}}{2}\langle \Gamma(B^0_s(t) \to f)\rangle\Big|_{t=0} = \frac{\tau_{B_s}}{2}\left(R^f_{\rm H} + R^f_{\rm L}\right). \tag{13}$$

By considering $t = 0$, the effect of B^0_s–$\bar{B}^0_s$ mixing is "switched off". The advantage of this definition is that it allows a straightforward comparison with the branching ratios of B^0_d or B^+_u mesons by means of the $SU(3)$ flavor symmetry. Using the relation

$$\mathrm{BR}\,(B_s \to f) = \left[\frac{1 - y_s^2}{1 + \mathcal{A}^f_{\Delta\Gamma}\, y_s}\right] \overline{\mathrm{BR}}\,(B_s \to f)\,, \tag{14}$$

the experimental branching ratio can be converted into the theoretical branching ratio.[21] While the decay width parameter y_s has already been measured, the observable $\mathcal{A}^f_{\Delta\Gamma}$ depends on the considered decay and generally involves non-perturbative parameters. As can be seen in Fig. 3, the differences between the two branching ratio concepts can be as large as $\mathcal{O}(10\%)$ for the measured value of y_s in Eq. (10).

In order to determine the process-dependent value of $\mathcal{A}^f_{\Delta\Gamma}$, typically theoretical assumptions have to be made, such as using the $SU(3)$ flavor symmetry in the case of non-leptonic B_s decays (for a compilation of results, see Ref. 21). For the extraction of the theoretical branching ratio, it is desirable to avoid theoretical input. This can be achieved by means of a measurement of the effective $B_s \to f$ decay lifetime:[21]

$$\tau_f \equiv \frac{\int_0^\infty t\,\langle\Gamma(B_s(t)\to f)\rangle\,dt}{\int_0^\infty \langle\Gamma(B_s(t)\to f)\rangle\,dt} = \frac{\tau_{B_s}}{1-y_s^2}\left[\frac{1+2\,\mathcal{A}^f_{\Delta\Gamma}y_s+y_s^2}{1+\mathcal{A}^f_{\Delta\Gamma}y_s}\right], \tag{15}$$

which yields

$$\mathrm{BR}\,(B_s\to f) = \left[2-\left(1-y_s^2\right)\frac{\tau_f}{\tau_{B_s}}\right]\overline{\mathrm{BR}}\,(B_s\to f)\,. \tag{16}$$

On the right-hand side of this expression, only quantities enter which can be measured. Once information on the effective decay lifetime is available, which requires a time-dependent measurement of the untagged B_s decay rate as can be seen in Eq. (15), Eq. (16) is advocated for the determination of theoretical branching ratios for particle listings by the Particle Data Group.[21] For a discussion of the branching ratio measurements of $B_s \to VV$ decays into two vector mesons in the presence of a sizeable value of $\Delta\Gamma_s$, such as $B_s \to J/\psi\phi$, $B_s \to K^{*0}\bar{K}^{*0}$ and $B_s \to D_s^{*+}D_s^{*-}$, the reader is referred to Refs. 21, 27, 28.

3. The $B_s^0 \to \mu^+\mu^-$ Observables

The subtleties discussed in the previous section apply also to the decay $B_s^0 \to \mu^+\mu^-$. In this case, the branching ratio serves as a sensitive probe for New Physics and it is essential – in view of the current experimental situation with branching ratio measurements falling into the SM regime – to assess the impact of the sizeable decay width difference $\Delta\Gamma_s$. As we will see below, this quantity offers – apart from the complication for the analysis of the branching ratio – a new observable to search for New Physics. The discussion in this section follows closely Ref. 22.

3.1. *Decay Amplitude*

The low-energy effective Hamiltonian describing the decay $\bar{B}_s^0 \to \mu^+\mu^-$ is given as follows:

$$\mathcal{H}_{\rm eff} = -\frac{G_{\rm F}}{\sqrt{2}\pi}V_{ts}^*V_{tb}\alpha\big[C_{10}O_{10}+C_SO_S+C_PO_P+C'_{10}O'_{10}+C'_SO'_S+C'_PO'_P\big], \tag{17}$$

where $G_{\rm F}$ is Fermi's constant and α denotes the QED fine structure constant. In the general Hamiltonian in (17), only four-fermion operators with non-vanishing

$\bar{B}_s^0 \to \mu^+\mu^-$ matrix elements are included. They take the following form:

$$\begin{array}{ll} O_{10} = (\bar{s}\gamma_\mu P_L b)(\bar{\ell}\gamma^\mu\gamma_5\ell), & O'_{10} = (\bar{s}\gamma_\mu P_R b)(\bar{\ell}\gamma^\mu\gamma_5\ell) \\ O_S = m_b(\bar{s}P_R b)(\bar{\ell}\ell), & O'_S = m_b(\bar{s}P_L b)(\bar{\ell}\ell) \\ O_P = m_b(\bar{s}P_R b)(\bar{\ell}\gamma_5\ell), & O'_P = m_b(\bar{s}P_L b)(\bar{\ell}\gamma_5\ell), \end{array} \tag{18}$$

where $P_{L,R} \equiv (1 \mp \gamma_5)/2$ and m_b denotes the b-quark mass. The Wilson coefficients C_i, C'_i encode the short-distance physics. In the SM, only the operator O_{10} contributes with a *real* coefficient $C_{10}^{\rm SM}$. The outstanding feature of the $\bar{B}_s^0 \to \mu^+\mu^-$ channel is the sensitivity to (pseudo-)scalar lepton densities, which are described by the $O_{(P)S}$, $O'_{(P)S}$ operators, having Wilson coefficients which are still largely unconstrained.[29,30]

In order to calculate the decay amplitude, it is convenient to go to the rest frame of the decaying $\bar{B}_s^0$ meson and to distinguish between the $\mu_{\rm L}^+\mu_{\rm L}^-$ and $\mu_{\rm R}^+\mu_{\rm R}^-$ helicity configurations which are related to each other through a CP transformation:

$$|(\mu_{\rm L}^+\mu_{\rm L}^-)_{\rm CP}\rangle \equiv (\mathcal{CP})|\mu_{\rm L}^+\mu_{\rm L}^-\rangle = e^{i\phi_{\rm CP}(\mu\mu)}|\mu_{\rm R}^+\mu_{\rm R}^-\rangle. \tag{19}$$

The $e^{i\phi_{\rm CP}(\mu\mu)}$ is a convention-dependent phase factor which cancels in the observables discussed below. The general expression for the decay amplitude (with $\eta_{\rm L} = +1$ and $\eta_{\rm R} = -1$) reads as

$$\begin{aligned} &A(\bar{B}_s^0 \to \mu_\lambda^+\mu_\lambda^-) = \langle\mu_\lambda^-\mu_\lambda^+|\mathcal{H}_{\rm eff}|\bar{B}_s^0\rangle = \\ &-\frac{G_{\rm F}}{\sqrt{2}\pi}V_{ts}^*V_{tb}\alpha F_{B_s}M_{B_s}m_\mu C_{10}^{\rm SM}e^{i\phi_{\rm CP}(\mu\mu)(1-\eta_\lambda)/2}\left[\eta_\lambda P + S\right]. \end{aligned} \tag{20}$$

Here the following combinations of Wilson coefficient functions were introduced:

$$P \equiv |P|e^{i\varphi_P} \equiv \frac{C_{10} - C'_{10}}{C_{10}^{\rm SM}} + \frac{M_{B_s}^2}{2\,m_\mu}\left(\frac{m_b}{m_b + m_s}\right)\left(\frac{C_P - C'_P}{C_{10}^{\rm SM}}\right) \stackrel{\rm SM}{\longrightarrow} 1 \tag{21}$$

$$S \equiv |S|e^{i\varphi_S} \equiv \sqrt{1 - 4\frac{m_\mu^2}{M_{B_s}^2}}\,\frac{M_{B_s}^2}{2\,m_\mu}\left(\frac{m_b}{m_b + m_s}\right)\left(\frac{C_S - C'_S}{C_{10}^{\rm SM}}\right) \stackrel{\rm SM}{\longrightarrow} 0, \tag{22}$$

where the $\varphi_{P,S}$ are CP-violating NP phases. As indicated, the P and S were introduced in such a way that they equal 1 and 0 in the SM case, respectively. In Eq. (20), F_{B_s} denotes the B_s decay constant as introduced in Eq. (1), M_{B_s} and m_μ are the B_s and muon masses, respectively, while m_s denotes the strange-quark mass.

3.2. *CP Asymmetries*

For the calculation of the CP asymmetries and the untagged rate of $B_s \to \mu^+\mu^-$, the following observable is required:[18]

$$\xi_\lambda \equiv -e^{-i\phi_s}\left[e^{i\phi_{\rm CP}(B_s)}\frac{A(\bar{B}_s^0 \to \mu_\lambda^+\mu_\lambda^-)}{A(B_s^0 \to \mu_\lambda^+\mu_\lambda^-)}\right], \tag{23}$$

which involves also the amplitude

$$A(B_s^0 \to \mu_\lambda^+ \mu_\lambda^-) = \langle \mu_\lambda^- \mu_\lambda^+ | \mathcal{H}_{\rm eff}^\dagger | B_s^0 \rangle. \tag{24}$$

Using $(\mathcal{CP})^\dagger(\mathcal{CP}) = \hat{1}$ and $(\mathcal{CP})|B_s^0\rangle = e^{i\phi_{\rm CP}(B_s)}|\bar{B}_s^0\rangle$ yields the expression

$$\begin{aligned} A(B_s^0 \to \mu_\lambda^+ \mu_\lambda^-) = &-\frac{G_{\rm F}}{\sqrt{2}\pi} V_{ts} V_{tb}^* \alpha f_{B_s} M_{B_s} m_\mu C_{10}^{\rm SM} \\ &\times e^{i[\phi_{\rm CP}(B_s) + \phi_{\rm CP}(\mu\mu)(1-\eta_\lambda)/2]} \left[-\eta_\lambda P^* + S^*\right]. \end{aligned} \tag{25}$$

The convention-dependent phases cancel in ξ_λ, which takes the form

$$\xi_\lambda = -\left[\frac{+\eta_\lambda P + S}{-\eta_\lambda P^* + S^*}\right], \tag{26}$$

satisfying the relation

$$\xi_{\rm L}\xi_{\rm R}^* = \xi_{\rm R}\xi_{\rm L}^* = 1. \tag{27}$$

The time-dependent CP asymmetry, which requires *tagging* to distinguish initially, i.e. at time $t = 0$, present B_s^0 and $\bar{B}_s^0$ mesons, is given by

$$\frac{\Gamma(B_s^0(t) \to \mu_\lambda^+\mu_\lambda^-) - \Gamma(\bar{B}_s^0(t) \to \mu_\lambda^+\mu_\lambda^-)}{\Gamma(B_s^0(t) \to \mu_\lambda^+\mu_\lambda^-) + \Gamma(\bar{B}_s^0(t) \to \mu_\lambda^+\mu_\lambda^-)} = \frac{C_\lambda \cos(\Delta M_s t) + S_\lambda \sin(\Delta M_s t)}{\cosh(y_s t/\tau_{B_s}) + \mathcal{A}_{\Delta\Gamma}^\lambda \sinh(y_s t/\tau_{B_s})}. \tag{28}$$

The observables entering this expressions do not depend on the decay constant F_{B_s}, in contrast to the branching ratio in (2), and read as follows:

$$C_\lambda \equiv \frac{1-|\xi_\lambda|^2}{1+|\xi_\lambda|^2} = -\eta_\lambda \left[\frac{2|PS|\cos(\varphi_P - \varphi_S)}{|P|^2 + |S|^2}\right] \quad \stackrel{\rm SM}{\longrightarrow} \quad 0 \tag{29}$$

$$S_\lambda \equiv \frac{2\,{\rm Im}\,\xi_\lambda}{1+|\xi_\lambda|^2} = \frac{|P|^2\sin(2\varphi_P - \phi_s^{\rm NP}) - |S|^2\sin(2\varphi_S - \phi_s^{\rm NP})}{|P|^2 + |S|^2} \quad \stackrel{\rm SM}{\longrightarrow} \quad 0 \tag{30}$$

$$\mathcal{A}_{\Delta\Gamma}^\lambda \equiv \frac{2\,{\rm Re}\,\xi_\lambda}{1+|\xi_\lambda|^2} = \frac{|P|^2\cos(2\varphi_P - \phi_s^{\rm NP}) - |S|^2\cos(2\varphi_S - \phi_s^{\rm NP})}{|P|^2 + |S|^2} \quad \stackrel{\rm SM}{\longrightarrow} \quad 1, \tag{31}$$

where also the corresponding SM values are given. The phase $\phi_s^{\rm NP}$ is the NP component of the B_s^0–$\bar{B}_s^0$ mixing phase

$$\phi_s = \phi_s^{\rm SM} + \phi_s^{\rm NP} = -2\lambda^2\eta + \phi_s^{\rm NP}. \tag{32}$$

It should be noted that

$$\mathcal{S}_{\mu\mu} \equiv S_\lambda \quad \text{and} \quad \mathcal{A}_{\Delta\Gamma}^{\mu\mu} \equiv \mathcal{A}_{\Delta\Gamma}^\lambda \tag{33}$$

are *independent* of the muon helicity λ. Neglecting the impact of $\Delta\Gamma_s$, CP asymmetries in $B_{s,d} \to \ell^+\ell^-$ decays were considered for various NP scenarios in the previous literature.[31–33]

Since it is difficult to measure the muon helicity, we consider the rate

$$\Gamma(B_s^0(t) \to \mu^+\mu^-) \equiv \sum_{\lambda={\rm L,R}} \Gamma(B_s^0(t) \to \mu_\lambda^+\mu_\lambda^-), \tag{34}$$

and in analogy for the CP-conjugate process. The corresponding CP-violating rate asymmetry takes the form

$$\frac{\Gamma(B_s^0(t)\to\mu^+\mu^-)-\Gamma(\bar{B}_s^0(t)\to\mu^+\mu^-)}{\Gamma(B_s^0(t)\to\mu^+\mu^-)+\Gamma(\bar{B}_s^0(t)\to\mu^+\mu^-)}=\frac{\mathcal{S}_{\mu\mu}\sin(\Delta M_s t)}{\cosh(y_s t/\tau_{B_s})+\mathcal{A}_{\Delta\Gamma}^{\mu\mu}\sinh(y_s t/\tau_{B_s})}, \tag{35}$$

where the $C_\lambda \propto \eta_\lambda$ terms entering Eq. (28) cancel. It would be most interesting to measure this CP asymmetry as a non-zero value would signal CP-violating NP phases, as will be discussed in detail below. Unfortunately, this is challenging in view of the tiny branching ratio and as tagging and time information are required.

3.3. *Untagged Rate and Branching Ratio*

The first measurements of the $B_s\to\mu^+\mu^-$ channel discussed in Section 1 concern the experimental branching ratio:

$$\overline{\rm BR}(B_s\to\mu^+\mu^-)\equiv\frac{1}{2}\int_0^\infty\langle\Gamma(B_s(t)\to\mu^+\mu^-)\rangle\,dt, \tag{36}$$

i.e. the time-integrated untagged rate, with

$$\begin{aligned}\langle\Gamma(B_s(t)\to\mu^+\mu^-)\rangle &\equiv \Gamma(B_s^0(t)\to\mu^+\mu^-)+\Gamma(\bar{B}_s^0(t)\to\mu^+\mu^-)\\ &\propto e^{-t/\tau_{B_s}}\left[\cosh(y_s t/\tau_{B_s})+\mathcal{A}_{\Delta\Gamma}^{\mu\mu}\sinh(y_s t/\tau_{B_s})\right].\end{aligned} \tag{37}$$

With the help of the relation

$$\mathrm{BR}(B_s\to\mu^+\mu^-)=\left[\frac{1-y_s^2}{1+\mathcal{A}_{\Delta\Gamma}^{\mu\mu}\,y_s}\right]\overline{\rm BR}(B_s\to\mu^+\mu^-), \tag{38}$$

we may convert the experimental branching ratio into the theoretical branching ratio, which refers to $t=0$. The observable $\mathcal{A}_{\Delta\Gamma}^{\mu\mu}$ depends on possible NP contributions and is hence unknown, thereby satisfying $\mathcal{A}_{\Delta\Gamma}^{\mu\mu}\in[-1,+1]$. Consequently, there are two options for dealing with the theoretical interpretation of the measured, time-integrated branching ratio:

(i) Add an extra error to the experimental branching ratio:

$$\Delta\mathrm{BR}(B_s\to\mu^+\mu^-)|_{y_s}=\pm y_s\overline{\rm BR}(B_s\to\mu^+\mu^-). \tag{39}$$

(ii) Use the SM value $\mathcal{A}_{\Delta\Gamma}^{\mu\mu}|_{\rm SM}=+1$ to calculate a *new SM reference value* for the comparison with the time-integrated experimental branching ratio $\overline{\rm BR}(B_s\to\mu^+\mu^-)$. To this end, $\mathrm{BR}(B_s\to\mu^+\mu^-)_{\rm SM}$ has to be rescaled by the factor $1/(1-y_s)$, which results in

$$\overline{\rm BR}(B_s\to\mu^+\mu^-)_{\rm SM}=(3.65\pm0.23)\times10^{-9}. \tag{40}$$

Once more and more data are collected and also the decay time information for the untagged data sample is used, the effective $B_s\to\mu^+\mu^-$ lifetime

$$\tau_{\mu\mu}\equiv\frac{\int_0^\infty t\,\langle\Gamma(B_s(t)\to\mu^+\mu^-)\rangle\,dt}{\int_0^\infty\langle\Gamma(B_s(t)\to\mu^+\mu^-)\rangle\,dt} \tag{41}$$

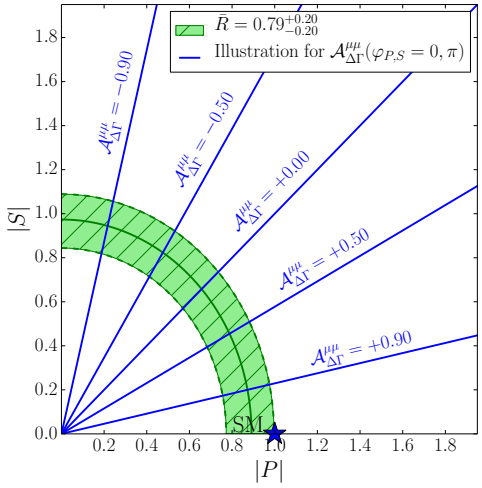

Fig. 4. The situation in the P–S plane, where the circular band corresponds to the allowed region following from (45), and contours for various values of the observable $\mathcal{A}^{\mu\mu}_{\Delta\Gamma}$ are shown, assuming no CP-violating NP phases φ_P and φ_S.

can be determined, which allows the extraction of the observable

$$\mathcal{A}^{\mu\mu}_{\Delta\Gamma} = \frac{1}{y_s}\left[\frac{(1-y_s^2)\tau_{\mu\mu} - (1+y_s^2)\tau_{B_s}}{2\tau_{B_s} - (1-y_s^2)\tau_{\mu\mu}}\right]. \tag{42}$$

The physics information encoded in $\tau_{\mu\mu}$ and $\mathcal{A}^{\mu\mu}_{\Delta\Gamma}$ is equivalent. Finally, using

$$\mathrm{BR}\left(B_s \to \mu^+\mu^-\right) = \left[2 - \left(1-y_s^2\right)\frac{\tau_{\mu\mu}}{\tau_{B_s}}\right]\overline{\mathrm{BR}}(B_s \to \mu^+\mu^-), \tag{43}$$

which involves only measurable quantities on the right-hand side, the theoretical $B_s \to \mu^+\mu^-$ branching ratio can be extracted directly from the data.[22] Authors have started to include the effect of $\Delta\Gamma_s$ in analyses of constraints on NP which are implied by the measured $\overline{\mathrm{BR}}(B_s \to \mu^+\mu^-)$ in the recent literature (see, for instance, Refs. 29 and 34–40).

4. Probing New Physics with $B_s^0 \to \mu^+\mu^-$

In the following, we assume that the B_s^0–$\bar{B}_s^0$ mixing phase ϕ_s will be precisely known by the time the $B_s \to \mu^+\mu^-$ observables introduced in the previous section can be measured,[41,42] which will allow the determination of the NP phase ϕ_s^{NP}.

In order to perform a test of the SM with the measurement of the $B_s \to \mu^+\mu^-$ branching ratio, it is useful to introduce the following ratio:[2,22]

$$\begin{aligned}\overline{R} &\equiv \frac{\overline{\mathrm{BR}}(B_s \to \mu^+\mu^-)}{\overline{\mathrm{BR}}(B_s \to \mu^+\mu^-)_{\mathrm{SM}}} = \left[\frac{1 + \mathcal{A}^{\mu\mu}_{\Delta\Gamma}\, y_s}{1+y_s}\right](|P|^2 + |S|^2) \\ &= \left[\frac{1 + y_s\cos(2\varphi_P - \phi_s^{\mathrm{NP}})}{1+y_s}\right]|P|^2 + \left[\frac{1 - y_s\cos(2\varphi_S - \phi_s^{\mathrm{NP}})}{1+y_s}\right]|S|^2. \end{aligned} \tag{44}$$

The current situation corresponds to

$$\overline{R} = 0.79 \pm 0.20. \tag{45}$$

Looking at Eq. (44), we observe that $\overline{R}$ does not allow a separation of the P and S contributions. Sizable NP contributions could be present in $B_s \to \mu^+\mu^-$, even if $\overline{R}$ is measured with a value close to $\overline{R}_{\rm SM} = 1$.

This situation can be resolved with the help of additional information, which is offered by the measurement of the effective lifetime $\tau_{\mu\mu}$ or – equivalently – the observable $\mathcal{A}^{\mu\mu}_{\Delta\Gamma}$:

$$|S| = |P|\sqrt{\frac{\cos(2\varphi_P - \phi_s^{\rm NP}) - \mathcal{A}^{\mu\mu}_{\Delta\Gamma}}{\cos(2\varphi_S - \phi_s^{\rm NP}) + \mathcal{A}^{\mu\mu}_{\Delta\Gamma}}}. \tag{46}$$

In Fig. 4, the current constraints in the $|P|$–$|S|$ plane are shown with an illustration of the contours following from a future measurement of $\mathcal{A}^{\mu\mu}_{\Delta\Gamma}$. In the calculation of the latter curves, it was assumed that there are no CP-violating NP phases φ_P and φ_S, as is the case, for instance, in NP models exhibiting MFV without flavour-blind phases.

In Ref. 2, detailed discussions of the regions in the $\overline{R}$–$\mathcal{A}^{\mu\mu}_{\Delta\Gamma}$ plane that are allowed by current data are given for a variety of scenarios:

- $P = 1 + \tilde{P}$ ($\tilde{P}$ free) and $S = 0$: the deviation of $\mathcal{A}^{\mu\mu}_{\Delta\Gamma}$ from its SM value $+1$ requires CP-violating NP phases. [Examples: CMFV, LHT, 4G, RSc, Z']
- $P = 1$ and S free: $\mathcal{A}^{\mu\mu}_{\Delta\Gamma}$ may differ from its SM value $+1$ without new CP-violating phases, with $\overline{R} \geq 1$. The experimental data have already quite some impact in this scenario. [Example: 2HDM (scalar H^0 dominance)]
- $P \pm S = 1$: the full range of $\mathcal{A}^{\mu\mu}_{\Delta\Gamma}$ can be accessed without new CP-violating phases, and the following lower bound arises:

$$\overline{\rm BR}(B_s \to \mu^+\mu^-) \geq \frac{1}{2}\,(1 - y_s)\,\overline{\rm BR}(B_s \to \mu^+\mu^-)_{\rm SM}. \tag{47}$$

  [Example: decoupled 2HDM/MSSM ($M_{H^0} \approx M_{A^0} \gg M_{h^0}$)]

In addition to the discussion of these general scenarios, also detailed analyses within specific NP models were performed in Ref. 2:

- Tree-level neutral gauge boson exchange, characterised by

$$\mathcal{L}_{\rm FCNC}(Z') = \left[\Delta_L^{sb}(Z')(\bar{s}\gamma_\mu P_L b) + \Delta_R^{sb}(Z')(\bar{s}\gamma_\mu P_R b)\right] Z'^{\mu}. \tag{48}$$

  Various scenarios can be distinguished: left-handed scheme (LHS) with complex $\Delta_L^{bs} \neq 0$ and $\Delta_R^{bs} = 0$, right-handed scheme (RHS) with complex $\Delta_R^{bs} \neq 0$ and $\Delta_L^{bs} = 0$, left-right symmetric scheme (LRS) with complex $\Delta_L^{bs} = \Delta_R^{bs} \neq 0$, left-right asymmetric scheme (ALRS) with complex $\Delta_L^{bs} = -\Delta_R^{bs} \neq 0$.
- Tree-level neutral (pseudo)scalar exchange:

$$\mathcal{L}_{\rm FCNC}(H) = \left[\Delta_L^{sb}(H)(\bar{s}P_L b) + \Delta_R^{sb}(H)(\bar{s}P_R b)\right] H. \tag{49}$$

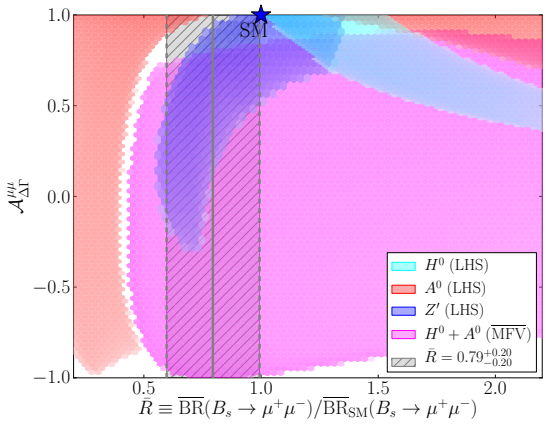

Fig. 5. Allowed regions in the $\overline{R}$–$\mathcal{A}^{\mu\mu}_{\Delta\Gamma}$ plane for various NP scenarios.[2]

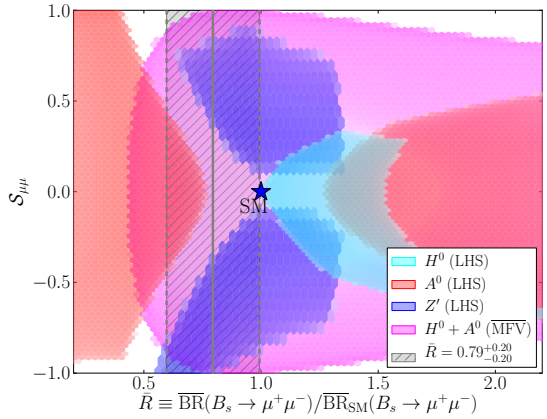

Fig. 6. Allowed regions in the $\overline{R}$–$\mathcal{S}_{\mu\mu}$ plane for various NP scenarios.[2]

- Tree-level neutral scalar+pseudoscalar exchange:

$$\begin{aligned}\mathcal{L}_{\mathrm{FCNC}}(H^0, A^0) = \; & \left[\Delta_L^{sb}(H^0)(\bar{s}P_L b) + \Delta_R^{sb}(H^0)(\bar{s}P_R b)\right] H^0 \\ & + \left[\Delta_L^{sb}(A^0)(\bar{s}P_L b) + \Delta_R^{sb}(A^0)(\bar{s}P_R b)\right] A^0. \end{aligned} \tag{50}$$

In the exploration of the allowed regions in observable space, it is important to take also experimental constraints on B_s^0–$\bar{B}_s^0$ mixing and other rare decays into account.

In Fig. 5, the constraints in the $\overline{R}$–$\mathcal{A}^{\mu\mu}_{\Delta\Gamma}$ plane are shown, involving only *untagged* observables of the $B_s \to \mu^+\mu^-$ channel. The allowed regions in this figure are complemented by those in Fig. 6, showing the situation in the $\overline{R}$–$\mathcal{S}_{\mu\mu}$ plane. Here *tagging* is required for the measurement of the CP asymmetry $\mathcal{S}_{\mu\mu}$, as can be seen

in Eq. (35). It is interesting to note the relation

$$|\mathcal{S}_{\mu\mu}|^2 + |\mathcal{A}^{\mu\mu}_{\Delta\Gamma}|^2 = 1 - \left[\frac{2|PS|\cos(\varphi_P - \varphi_S)}{|P|^2 + |S|^2}\right]^2, \tag{51}$$

which illustrates the sensitivity to CP-violating NP phases.

5. Summary and Outlook

We live in exciting times for studies of leptonic rare $B_{(s)}$-meson decays. Concerning $B_d \to \mu^+\mu^-$, the average of the CMS and LHCb results for the branching ratio is given by $\left(3.6^{+1.6}_{-1.4}\right) \times 10^{-10}$ while the SM prediction reads $(1.06 \pm 0.09) \times 10^{-10}$. The large central value of the experimental average would immediately imply NP and would rule out models with MFV. But the large error does unfortunately not allow us to draw conclusions at this point. It will be very interesting to monitor the future evolution of the data.

Concerning $B_s \to \mu^+\mu^-$, there is finally evidence for this channel in the data of the CMS and LHCb collaborations. The corresponding LHC average for the measured branching ratio is given by $\overline{\rm BR}(B_s \to \mu^+\mu^-) = (2.9 \pm 0.7) \times 10^{-9}$. This result falls well into the SM regime although the error is still sizeable.

The interpretation of this measurement is affected by a – seemingly – unrelated topic, which is the recent development that a non-vanishing value of the B_s decay width difference $\Delta\Gamma_s$ was established by the LHCb collaboration. In view of this result, special care has to be taken when dealing with branching ratios of B_s decays, distinguishing in particular between the "experimental" and "theoretical" branching ratios. Apart from this complication, $\Delta\Gamma_s$ offers new observables which are encoded in the effective lifetimes of B_s decays. The most relevant application concerns the search for NP with $B_s \to \mu^+\mu^-$.

The SM reference value for the comparison with the time-integrated experimental branching ratio including the $\Delta\Gamma_s$ effects is given as follows:

$$\overline{\rm BR}(B_s \to \mu^+\mu^-)_{\rm SM} = (3.65 \pm 0.23) \times 10^{-9}, \tag{52}$$

using the most recent theoretical analysis of Refs. 5, 6, 7.

Apart from a more precise measurement of $\overline{\rm BR}(B_s \to \mu^+\mu^-)$, the next conceptual step is the analysis of the *time-dependent* untagged $B_s \to \mu^+\mu^-$ rate and the determination of the effective lifetime $\tau_{\mu\mu}$. The sizeable $\Delta\Gamma_s$ offers access to $\mathcal{A}^{\mu\mu}_{\Delta\Gamma}$, which is a new *theoretically clean* observable to search for NP. In contrast to the branching ratio, the dependence on the B_s decay constant F_{B_s} cancels out. Interestingly, $\mathcal{A}^{\mu\mu}_{\Delta\Gamma}$ may reveal NP effects even if the branching ratio is found close to the SM prediction. Using in addition tagging information to distinguish between initially present B^0_s or $\bar{B}^0_s$ mesons, the CP asymmetry $\mathcal{S}_{\mu\mu}$ can be extracted from the time-dependent rates.

Thanks to still largely unconstrained (pseudo-)scalar operators $O_{(P)S}$, $O'_{(P)S}$ there is still sizeable space for NP to manifest itself in these observables. Correla-

tions between $\overline{R}$, $\mathcal{A}_{\Delta\Gamma}^{\mu\mu}$ and $\mathcal{S}_{\mu\mu}$ allow us to distinguish between different NP scenarios, with their specific effective operators and CP-violating phases. A particularly exciting scenario would be the detection of sources of CP violation originating from physics beyond the SM. The new $B_s \to \mu^+\mu^-$ observables offer new studies for the LHC upgrade physics programme and may allow us to eventually reveal NP in $B_s \to \mu^+\mu^-$, one of the rarest and most fascinating decays Nature has to offer.

Acknowledgments

I would like to thank my PhD students and colleagues for the enjoyable collaboration on topics discussed above, and Rob Knegjens for numerical updates. I am very grateful to Harald Fritzsch and his co-organizers for inviting me to this excellent and most enjoyable workshop on Flavor Physics and Mass Generation and for their kind hospitality in Singapore.

References

1. A. J. Buras, J. Girrbach, D. Guadagnoli and G. Isidori, Eur. Phys. J. C **72**, 2172 (2012) [arXiv:1208.0934 [hep-ph]].
2. A. J. Buras, R. Fleischer, J. Girrbach and R. Knegjens, JHEP **1307**, 77 (2013) [arXiv:1303.3820 [hep-ph]].
3. R. J. Dowdall *et al.* [HPQCD Collaboration], Phys. Rev. Lett. **110**, 222003 (2013) [arXiv:1302.2644 [hep-lat]].
4. Y. Amhis *et al.* [Heavy Flavor Averaging Group Collaboration], *Averages of B-Hadron, C-Hadron, and tau-lepton properties as of early 2012*, arXiv:1207.1158 [hep-ex]; for updates, see http://www.slac.stanford.edu/xorg/hfag/
5. C. Bobeth, M. Gorbahn, T. Hermann, M. Misiak, E. Stamou and M. Steinhauser, Phys. Rev. Lett. **112**, 101801 (2014) [arXiv:1311.0903 [hep-ph]].
6. C. Bobeth, M. Gorbahn and E. Stamou, Phys. Rev. D **89**, 034023 (2014) [arXiv:1311.1348 [hep-ph]].
7. T. Hermann, M. Misiak and M. Steinhauser, JHEP **1312**, 097 (2013) [arXiv:1311.1347 [hep-ph]].
8. D. M. Straub, arXiv:1012.3893 [hep-ph].
9. A. J. Buras and J. Girrbach, Acta Phys. Polon. B **43**, 1427 (2012) [arXiv:1204.5064 [hep-ph]].
10. T. Aaltonen *et al.* [CDF Collaboration], Phys. Rev. D **87**, 072003 (2013) [arXiv:1301.7048 [hep-ex]].
11. V. M. Abazov *et al.* [D0 Collaboration], Phys. Rev. D **87**, 072006 (2013) [arXiv:1301.4507 [hep-ex]].
12. G. Aad *et al.* [ATLAS Collaboration], Phys. Lett. B **713**, 387 (2012) [arXiv:1204.0735 [hep-ex]]; ATLAS-CONF-2013-076 (2013).
13. S. Chatrchyan *et al.* [CMS Collaboration], Phys. Rev. Lett. **111**, 101804 (2013) [arXiv:1307.5025 [hep-ex]].
14. R. Aaij *et al.* [LHCb Collaboration], Phys. Rev. Lett. **111**, 101805 (2013) [arXiv:1307.5024 [hep-ex]].
15. The CMS and LHCb Collaborations, CMS-PAS-BPH-13-007, LHCb-CONF-2013-012 (2013).
16. R. Fleischer, N. Serra and N. Tuning, Phys. Rev. D **82**, 034038 (2010) [arXiv:1004.3982 [hep-ph]]; Phys. Rev. D **83**, 014017 (2011) [arXiv:1012.2784 [hep-ph]].

17. J. A. Bailey, A. Bazavov, C. Bernard, C. M. Bouchard, C. DeTar, D. Du, A. X. El-Khadra and J. Foley *et al.*, Phys. Rev. D **85**, 114502 (2012) [Erratum-ibid. D **86**, 039904 (2012)] [arXiv:1202.6346 [hep-lat]].
18. R. Fleischer, Phys. Rept. **370**, 537 (2002) [hep-ph/0207108].
19. A. Lenz, *Theoretical update of B-Mixing and Lifetimes*, arXiv:1205.1444 [hep-ph].
20. R. Aaij *et al.* [LHCb Collaboration], Phys. Rev. D **87**, 112010 (2013) [arXiv:1304.2600 [hep-ex]].
21. K. De Bruyn, R. Fleischer, R. Knegjens, P. Koppenburg, M. Merk and N. Tuning, Phys. Rev. D **86**, 014027 (2012) [arXiv:1204.1735 [hep-ph]].
22. K. De Bruyn, R. Fleischer, R. Knegjens, P. Koppenburg, M. Merk, A. Pellegrino and N. Tuning, Phys. Rev. Lett. **109**, 041801 (2012) [arXiv:1204.1737 [hep-ph]].
23. I. Dunietz, R. Fleischer and U. Nierste, Phys. Rev. D **63**, 114015 (2001) [hep-ph/0012219].
24. R. Fleischer, Eur. Phys. J. C **10**, 299 (1999) [hep-ph/9903455].
25. R. Fleischer, Phys. Lett. B **459**, 306 (1999) [hep-ph/9903456].
26. S. Faller, R. Fleischer and T. Mannel, Phys. Rev. D **79**, 014005 (2009) [arXiv:0810.4248 [hep-ph]].
27. R. Aaij *et al.* [LHCb Collaboration], Phys. Lett. B **709**, 50 (2012) [arXiv:1111.4183 [hep-ex]].
28. S. Descotes-Genon, J. Matias and J. Virto, Phys. Rev. D **85**, 034010 (2012) [arXiv:1111.4882 [hep-ph]].
29. W. Altmannshofer and D. M. Straub, JHEP **1208**, 121 (2012) [arXiv:1206.0273 [hep-ph]].
30. W. Altmannshofer, PoS Beauty **2013**, 024 (2013) [arXiv:1306.0022 [hep-ph]].
31. C.-S. Huang and W. Liao, Phys. Lett. B **525**, 107 (2002) [hep-ph/0011089]; Phys. Lett. B **538**, 301 (2002) [hep-ph/0201121].
32. A. Dedes and A. Pilaftsis, Phys. Rev. D **67**, 015012 (2003) [hep-ph/0209306].
33. P. H. Chankowski, J. Kalinowski, Z. Was and M. Worek, Nucl. Phys. B **713**, 555 (2005) [hep-ph/0412253].
34. X. -Q. Li, J. Lu and A. Pich, JHEP **1406**, 022 (2014) [arXiv:1404.5865 [hep-ph]].
35. W. Altmannshofer, M. Carena, N. R. Shah and F. Yu, JHEP **1301**, 160 (2013) [arXiv:1211.1976 [hep-ph]].
36. A. J. Buras, F. De Fazio and J. Girrbach, JHEP **1302**, 116 (2013) [arXiv:1211.1896 [hep-ph]].
37. O. Buchmueller, R. Cavanaugh, M. Citron, A. De Roeck, M. J. Dolan, J. R. Ellis, H. Flacher and S. Heinemeyer *et al.*, Eur. Phys. J. C **72**, 2243 (2012) [arXiv:1207.7315].
38. T. Hurth and F. Mahmoudi, Nucl. Phys. B **865** (2012) 461 [arXiv:1207.0688 [hep-ph]].
39. D. Becirevic, N. Kosnik, F. Mescia and E. Schneider, Phys. Rev. D **86**, 034034 (2012) [arXiv:1205.5811 [hep-ph]].
40. F. Mahmoudi, S. Neshatpour and J. Orloff, JHEP **1208**, 092 (2012) [arXiv:1205.1845 [hep-ph]].
41. G. Borissov, R. Fleischer and M.-H. Schune, Ann. Rev. Nucl. Part. Sci. **63**, 205 (2013) [arXiv:1303.5575 [hep-ph]].
42. W. Hulsbergen, Mod. Phys. Lett. A **28**, 1330023 (2013) [arXiv:1306.6474 [hep-ph]].